

# Drug Repositioning and Pharmacophore Identification in the Discovery of Hookworm MIF Inhibitors

Yoonsang Cho,<sup>1,6</sup> Jon J. Vermeire,<sup>2,6</sup> Jane S. Merkel,<sup>5</sup> Lin Leng,<sup>3</sup> Xin Du,<sup>3</sup> Richard Bucala,<sup>3,4</sup> Michael Cappello,<sup>2,\*</sup> and Elias Lolis<sup>1,4,\*</sup>

<sup>1</sup>Department of Pharmacology

<sup>2</sup>Department of Pediatrics

<sup>3</sup>Department of Internal Medicine

<sup>4</sup>Yale Cancer Center

Yale University School of Medicine, New Haven, CT 06520, USA

<sup>5</sup>Small Molecular Discovery Center, Yale University, New Haven, CT 06511, USA

<sup>6</sup>The authors equally contributed in this work

\*Correspondence: michael.cappello@yale.edu (M.C.), elias.lolis@yale.edu (E.L.)

DOI 10.1016/j.chembiol.2011.07.011

## SUMMARY

The screening of bioactive compound libraries can be an effective approach for repositioning FDA-approved drugs or discovering new pharmacophores. Hookworms are blood-feeding, intestinal nematode parasites that infect up to 600 million people worldwide. Vaccination with recombinant *Ancylostoma ceylanicum* macrophage migration inhibitory factor (rAceMIF) provided partial protection from disease, thus establishing a “proof-of-concept” for targeting AceMIF to prevent or treat infection. A high-throughput screen (HTS) against rAceMIF identified six AceMIF-specific inhibitors. A nonsteroidal anti-inflammatory drug (NSAID), sodium meclofenamate, could be tested in an animal model to assess the therapeutic efficacy in treating hookworm disease. Furosemide, an FDA-approved diuretic, exhibited submicromolar inhibition of rAceMIF tautomerase activity. Structure-activity relationships of a pharmacophore based on furosemide included one analog that binds similarly to the active site, yet does not inhibit the Na-K-Cl symporter (NKCC1) responsible for diuretic activity.

## INTRODUCTION

Hookworms are hematophagous, intestinal nematodes that exact a particularly devastating toll on young children and women of childbearing age by causing severe anemia and protein malnutrition. The majority of human hookworm infections are caused by *Ancylostoma duodenale*, *A. ceylanicum*, and *Necator americanus* (Bungiro and Cappello, 2004; Hotez et al., 2004). For each hookworm species, the life cycle begins when eggs are excreted in the feces of an infected individual onto warm, moist soil. The eggs hatch, releasing a first stage hookworm larva (L1), which undergoes successive molts to the infec-

tive third (L3) stage. Infectious L3 invade host skin and migrate to the lungs via the vasculature. After breaking out of the alveolar spaces and ascending the bronchial tree, the larvae are coughed up and swallowed by the host. Upon reaching the small intestine, the larvae molt to become adult worms, where they attach to the intestinal mucosa, ingest blood and tissue and begin to produce eggs. In heavily infected individuals with low dietary iron intake, the associated blood loss can rapidly lead to chronic hookworm disease, characterized by severe anemia, malnutrition, and growth/cognitive delay in children (Stephenson, et al., 2000). Nearly 600 million people are infected by hookworms, virtually all of whom live in resource-limited countries (Bethony et al., 2006; de Silva et al., 2003). Although treatment for hookworm disease is available, there is concern about drug resistance and the lack of late-stage development of novel therapeutics (Albonico et al., 2004). In addition, there are commercial challenges in supporting drug development for this parasitic disease. Drug repositioning is an effective mechanism to meet these challenges if there are currently used drugs that possess anthelmintic activity.

Macrophage migration inhibitory factor (MIF) is a mammalian cytokine involved in innate and adaptive immunity that plays multiple roles in the inflammatory response (Guo et al., 2009; Roger et al., 2001). MIF functions by activating the CD74/CD44 receptor complex, which signals through a Src kinase, resulting in the phosphorylation of the ERK-1/2, production of PGE<sub>2</sub>, and counter-regulation of corticosteroid activity, among other intracellular signaling events (Leng et al., 2003; Lolis 2001; Shi et al., 2006). MIF has also been shown to activate the chemokine receptors CXCR2 and CXCR4, and has a role in the development of atherosclerosis (Bernhagen et al., 2007). In contrast to most other cytokines, MIF is present in the cytosol and is released upon cellular stimulation (Kleemann et al., 2000; Merk et al., 2009). Also, MIF is expressed in a wide range of mammalian tissue and cell types as well as across a wide range of taxa including both free-living and parasitic nematodes (Esumi et al., 1998; Leng et al., 2003; Sato et al., 2003; Vermeire et al., 2008). Finally, structural studies reveal that MIF forms a homotrimer with three catalytic sites, each between two subunits, with structural similarity to two microbial enzymes—4-oxalocrotonate tautomerase and

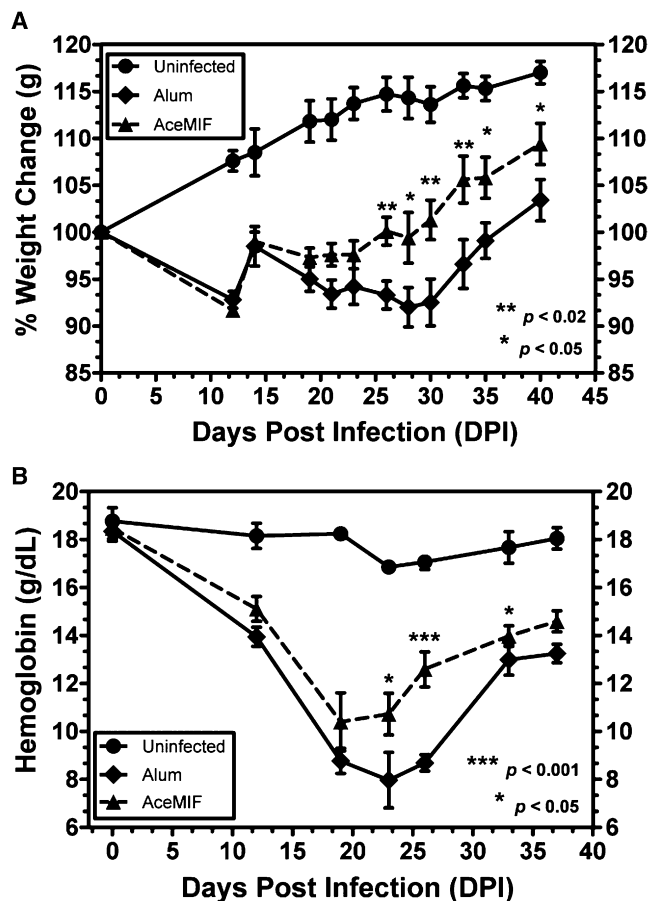


**Figure 1. Immunization of Hamsters with Recombinant AceMIF Followed by Challenge with *Ancylostoma Ceylanicum* Hookworms** Hamsters (5/group) were immunized subcutaneously with 100  $\mu$ g rAceMIF in the adjuvant alum, whereas controls received alum only. After boosting twice with 50  $\mu$ g of rAceMIF, animals were challenged with 100 *A. ceylanicum* infective larvae and monitored for 40 days. As shown in (A), immunization of hamsters with rAceMIF was associated with partial protection from hookworm-associated growth delay, with significantly higher body weights noted at days 26–40 post infection ( $p < 0.03$ ) compared with controls. In (B), immunized animals also exhibited less severe anemia after challenge infection, with higher blood hemoglobin levels from days 23–33 postinfection ( $p < 0.05$ ).

5-carboxymethyl-2-hydroxy-muconate isomerase (Subramanya et al., 1996; Sun et al., 1996; Suzuki et al., 1996). MIF has tautomerase activity on “model” substrates such as a 2-carboxy-2,3-dihydroindole-5,6-quinone (*L*-dopachrome) and hydroxyphenylpyruvate (HPP) (Rosengren et al., 1996, 1997). Small molecule binding within the active site of mammalian MIF active site reduces cellular (Lubetsky et al., 2002; Swope et al., 1998) and in vivo biological activity, providing a therapeutic effect in a number of diseases in mouse models including sepsis, colitis, and lupus among others (Crichlow et al., 2007; Dagia et al., 2009; Leng et al., 2011).

In our previous work, the cDNA of a MIF homolog from *A. ceylanicum* (AceMIF) was cloned and the recombinant protein was expressed and functionally characterized, and its three-dimensional structure determined by X-ray crystallography (Cho et al., 2007). In vitro experiments revealed AceMIF has tau-

tomerase activity and binds the MIF receptor, CD74, suggesting a role in modulating host immune responses to hookworm infection. Importantly, an inhibitor of human MIF, (S,R)-3-(4-hydroxyphenyl)-4,5-dihydro-5-isoxazole acetic acid methyl ester (ISO-1), did not inhibit AceMIF tautomerase or chemoattractant activities, suggesting that differences in the enzymatic sites might allow for identification of specific inhibitors of AceMIF.

Recently the issue of repositioning FDA-approved drugs for new indications has gained significant attention as a result of the time and cost necessary in bringing a novel drug into clinical use (Chong and Sullivan, 2007). Here we report the results of a high throughput screening (HTS) of a clinically active, small molecule library against AceMIF on the basis of the inhibition of tautomerase activity. We tested the effect of each inhibitor in three assays to choose a compound for further therapeutic development: inhibition of (1) catalytic activity, (2) binding to the MIF receptor, CD74, and (3) AceMIF-mediated monocyte migration. We also examined the toxicity of the compounds in an ex vivo worm-killing assay. Analyses of the results allowed us to choose one inhibitor compound with activities in assays 1–3 for repositioning and another inhibitor with activities against all four assays for further structure-activity and crystallographic studies, forming the basis for future structure-based drug design and in vivo studies with a hamster model of hookworm disease (Bungiro et al., 2001; Cappello et al., 2006; Garside and Behnke 1989).

## RESULTS

### AceMIF Immunization

To test whether neutralization of AceMIF would impact hookworm-induced pathogenesis, Syrian hamsters were immunized with rAceMIF and followed for changes in body weight and blood hemoglobin levels after hookworm infection. Hamsters were immunized subcutaneously with 100  $\mu$ g of rAceMIF in alum adjuvant, whereas controls received alum only. After boosting (50  $\mu$ g of rAceMIF 2X), animals were challenged with 100 *A. ceylanicum* infective larvae and monitored for 40 days. As shown in Figure 1A, immunization of hamsters with rAceMIF was associated with partial protection from hookworm-associated growth delay and with significantly higher body weights noted at days 26–40 postinfection ( $p < 0.03$ ) compared with controls. Immunized animals also exhibited less severe anemia after challenge infection, with higher blood hemoglobin levels noted from days 23–33 postinfection (Figure 1B,  $p < 0.05$ ). The demonstration that vaccination confers partial protection from clinical symptoms of hookworm-associated disease (weight loss and anemia) suggests that AceMIF, which is secreted by adult *A. ceylanicum*, is an important virulence factor that plays a role in pathogenesis. It also suggests that AceMIF is accessible by antibodies in the bloodstream of infected animals and therefore could be targeted using small molecule inhibitors. In previous studies, inhibitors targeting the catalytic site of human MIF were therapeutic in vivo, further providing a rationale for inhibiting this site of AceMIF (Crichlow, et al., 2007; Dagia et al., 2009; Leng et al., 2011).

### Inhibitors from a Chemical Library

A HTS assay of *L*-dopachrome tautomerase activity ( $Z'$  [Equation S1] value  $> 0.8$ ) was developed for AceMIF using an

automatic liquid handler and plate reader to screen a small chemical library composed of FDA-approved drugs and other bioactive compounds (GenPlus, MicroSource, Gaylordville, CT) (Zhang et al., 1999). The rationale for developing this assay was based on previous studies that identified small molecules that bind the MIF active site and have proven to have therapeutic effect in animal models of disease (Crichlow et al., 2007; Dagia et al., 2009; Leng et al., 2011). Eleven compounds that inhibited AceMIF *L*-dopachrome tautomerase activity by more than 60% relative to controls in the HTS assay were selected and purchased for laboratory studies. Five of those that also inhibited human MIF or were false positives were removed from further characterization. Cross-reactivity of the six remaining AceMIF inhibitors (Table 1) was studied using the HPP tautomerase assay against human MIF and the  $K_i$ 's were 3–104-fold greater than AceMIF (see Table S1 available online). Human MIF-mediated peripheral blood mononuclear cell (PBMC) migration was not significantly inhibited by any compound. Interaction of human MIF with sCD74 was also not inhibited by any of the compounds.

Among these six compounds were: pyrantel pamoate (compound 4) and hexylresorcinol (compound 6), two compounds with anthelmintic properties; sodium meclofenamate (compound 1), a NSAID; furosemide (compound 2), a diuretic used to treat hypertension and heart failure; hydroxyzine pamoate (compound 3), an anti-anxiety medicine; and cobalamine (compound 5). We also performed a meta-analysis of 15 unrelated screens performed at the Yale Center for Proteomics and Genomics to characterize the specificity of the GenPlus library. Hexachlorophene was common in six different assays, including MIF, and was excluded from further studies with AceMIF. Of the compounds, 1, 2, 4, 5, and 6 were common in another screen for antioxidants. Compound 3 was common in two screens (Supplemental Experimental Procedures).

### Kinetic Properties of the Inhibitors

For extensive kinetic studies, HPP was used as a substrate instead of *L*-dopachrome, which is stable for only 20–30 min at ambient temperatures. Initial velocities of AceMIF tautomerase activity with three different inhibitor concentrations and HPP concentrations ranging from 0.01–2 mM were measured and analyzed to determine the inhibition type using Lineweaver-Burk plot analysis. In two recent studies, inhibitors were found to bind to an allosteric site adjacent to the active site and function as noncompetitive inhibitors (Cho et al., 2010; McLean et al., 2010). Representative graphs of a competitive, noncompetitive, and mixed inhibition are shown in Figures 2A–2C, respectively. A complete summary of  $K_i$ 's and inhibition types of all the inhibitors is listed in Table 1. Compounds 1, 2, and 4 are competitive inhibitors, with  $K_i$ 's in the sub- to micromolar range. Compounds 3 ( $K_i$  5.71  $\mu$ M) and 6 ( $K_i$  136.6  $\mu$ M) are both mixed inhibitors with varied  $K_i$ 's. Compound 5 was determined to be a noncompetitive inhibitor of AceMIF tautomerase activity and had a  $K_i$  of 124.4  $\mu$ M.

### Inhibition of AceMIF-Induced Chemotaxis

Chemotaxis assays with human PBMCs were performed at a single concentration of AceMIF with an excess of each compound (Figure 2D and Table 2). Interestingly, the antichemotactic activity of inhibitor compounds did not correlate with the potency of enzymatic inhibition. For example, compound 5 ( $K_i$

of 124.4  $\mu$ M) was a more potent antichemotactic agent than compounds 2, 3, and 4, which had  $K_i$ 's from 0.56–8.16  $\mu$ M. It is clear from Figure 2D that the type of inhibition also bears no relevance to the potency of antichemotactic activity because competitive, noncompetitive, and mixed inhibitors (compounds 1, 2, 4, 5, and 6) are all potent inhibitors of AceMIF-mediated monocyte chemotaxis. For compound 2, a dose-dependent inhibition assay was performed to estimate an  $IC_{50}$  value, which was approximately 1  $\mu$ M (Figure S1).

### Inhibition of AceMIF Binding to the Human CD74 Receptor

AceMIF interacts with the human MIF receptor CD74, presumably to modulate and potentially evade the host immune response (Cho et al., 2007). To determine whether any of the inhibitors block the binding of AceMIF to CD74, we used the same method as previously described to detect interactions with the immobilized soluble extracellular domain (residues 73–232) of CD74 (sCD74) (Leng et al., 2003). Compounds 2, 4, and 6 specifically interfered with AceMIF interactions with sCD74 at submicromolar  $IC_{50}$ 's (Table 1). A representative dose-response graph of compound 2 is shown in Figure 2E.

### Worm-Killing Assays

The anthelmintic activity of each of the inhibitors was tested against *A. ceylanicum* in an ex vivo worm-killing assay (Cappello et al., 2006). The rationale for these experiments was based on the presence of AceMIF in homogenates of *L3* larvae and adult *A. ceylanicum* (Cho et al., 2007), and that AceMIF may serve a worm-specific function(s) in the absence of host immune effectors, similar to that of human MIF (Mitchell et al., 2002). These experiments were also important in evaluating the nematocidal potential of each compound for future in vivo studies. Survival curves of AceMIF inhibitor-treated worms were significantly different from control worms treated with dimethyl sulfoxide (DMSO) alone (Table 1 and Figure 2F; compound 2,  $p = 0.0007$ ; compound 3,  $p = 0.0005$ ; compound 4,  $p = 0.0023$ ). However, survival curves of these compounds were not significantly different from each other. Compounds 2, 3, and 4 inhibited survival with 40%–50% worm-killing activity. All other compounds, including compound 1, the most potent enzymatic inhibitor, had worm-killing activity of 0%–15%, indicating that the blocking AceMIF active site is insufficient to kill hookworms ex vivo.

### Structure-Activity Relationships of Compound 2

Compound 2 exhibited the best combination of inhibitory activities—submicromolar for both the  $K_i$  for enzyme activity (binding to the AceMIF active site) and  $IC_{50}$  for CD74 receptor binding,  $IC_{50}$  of 1  $\mu$ M in monocyte chemotaxis experiments, and the largest effect in the worm-killing assay. Therefore, compound 2 was selected for further study. To investigate the contribution of each functional group of compound 2 in its inhibitory effect, structurally similar molecules were selected from a search of PubChem (<http://pubchem.ncbi.nlm.nih.gov/>) and assayed for comparison. Chemical structures and kinetic parameters of these structural analogs are shown in Table 1. Compound 9 (2-(furan-2-ylmethylamino) benzoic acid) and compound 2 have furfurylamine at the R1 position and have relatively low  $K_i$  values compared with compound 7 (4-chloro-5-(furan-2-ylmethylsulfamoyl)-2-piperidin-1-ylbenzoic

**Table 1. AceMIF Inhibitors Identified from HTS and Structural Similarity Search**

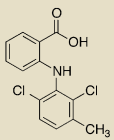
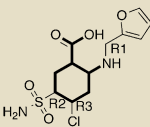
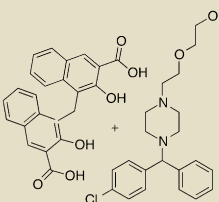
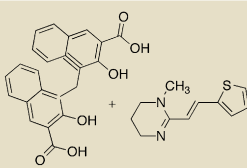
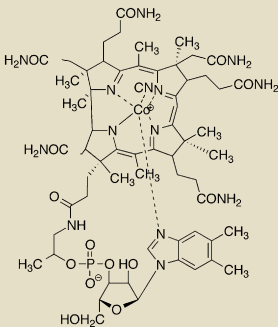
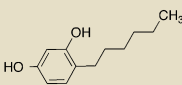
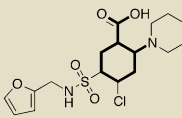
No	Structure	Tautomerase activity inhibition ( $\mu\text{M}$ )	PBMC migration inhibition (%)	CD74 binding inhibition ( $\mu\text{M}$ ) <sup>a</sup>	Worm-killing (%)
1		0.47(C)	100	34%	0
2		0.56(C)	89	0.33	50
3		5.71(M)	7	25%	50
4		8.16(C)	76	0.09	40
5		124.4(NC)	94	6%	0
6		136.6(M)	57	0.66	0
7		247.0(NC)	42	38%	0

Table 1. Continued

No	Structure	Tautomerase activity inhibition ( $\mu\text{M}$ )	PBMC migration inhibition (%)	CD74 binding inhibition ( $\mu\text{M}$ ) <sup>a</sup>	Worm-killing (%)
8		44.0(NC)	82	3.3	0
9		2.37(C)	82	15%	0
10		24.8(C)	35	9%	0
11		5.0(C)	19	2%	0
12		7.7(C)	50	10%	0
13		57.3(M)	26	21%	0

Six AceMIF inhibitors (compounds 1–6) were identified from the GenPlus small molecule library and seven structural analogs (compounds 7–13) of compound 2 were additionally searched from the PubChem database. All compounds were assayed for the inhibition of HPP tautomerase activity ( $K_i$ ) (inhibition types: C, competitive; M, mixed; NC, noncompetitive), PBMC migration (percent inhibition at 10  $\mu\text{M}$ ) and CD74 binding of AceMIF  $\text{IC}_{50}$ , and for worm-killing activity.

<sup>a</sup> Maximum percentile inhibition is listed due to the limited solubility of the compound.

acid), which has piperidine at the same position, and compound 8 (4-chloro-N-(furan-2-ylmethyl)-3-[methyl(phenyl)sulfamoyl]benzamide), which has no R1 group. This implies that the furfurylamine group plays an important role in interacting with AceMIF, and its affinity is significantly reduced when its position is changed to R2 as in compound 7.

Seven structural analogs of compound 2 were tested in the CD74 capture assay, PBMC migration assay, and ex vivo worm survival assay to determine their activities relative to compound 2 (Table 1). Compound 8 significantly inhibited the interaction of AceMIF with CD74 ( $\text{IC}_{50}$  of 3.3  $\mu\text{M}$ ), whereas compounds 7 and 9 inhibited only 38% and 15% of AceMIF-CD74 binding, respectively. In the PBMC migration assay, compounds 8 and 9 were similarly active in inhibiting AceMIF-mediated monocyte migration relative to compound 2, and compound 7, which is missing a furfurylamine group, was only half as active as the parent

compound. Interestingly, none of the structural analogs of compound 2 possessed worm-killing activity. Compound 10 has two methyl groups at R1 position instead of a furfuryl group and two methyl ethers at R2 and R3 positions.

The structural differences in the furosemide analogs caused significant changes in their ability to inhibit AceMIF tautomerase activity. For example, the only chemical difference between compounds 9 and 11 is the replacement of a methylene group with a carbonyl oxygen next to the anthranilate nitrogen to form a peptide bond (of compound 11), resulting in a 4-fold and 9-fold higher  $K_i$ , respectively, compared with compound 2 ( $K_i$  0.56  $\mu\text{M}$ ). Compound 12 is structurally similar to compound 11 but has an extra methyl group attached to a ring carbon of the furan group. This difference results in a 14-fold higher  $K_i$  value compared with that of compound 2. Replacement of the secondary amine linker with a methylated tertiary amine in



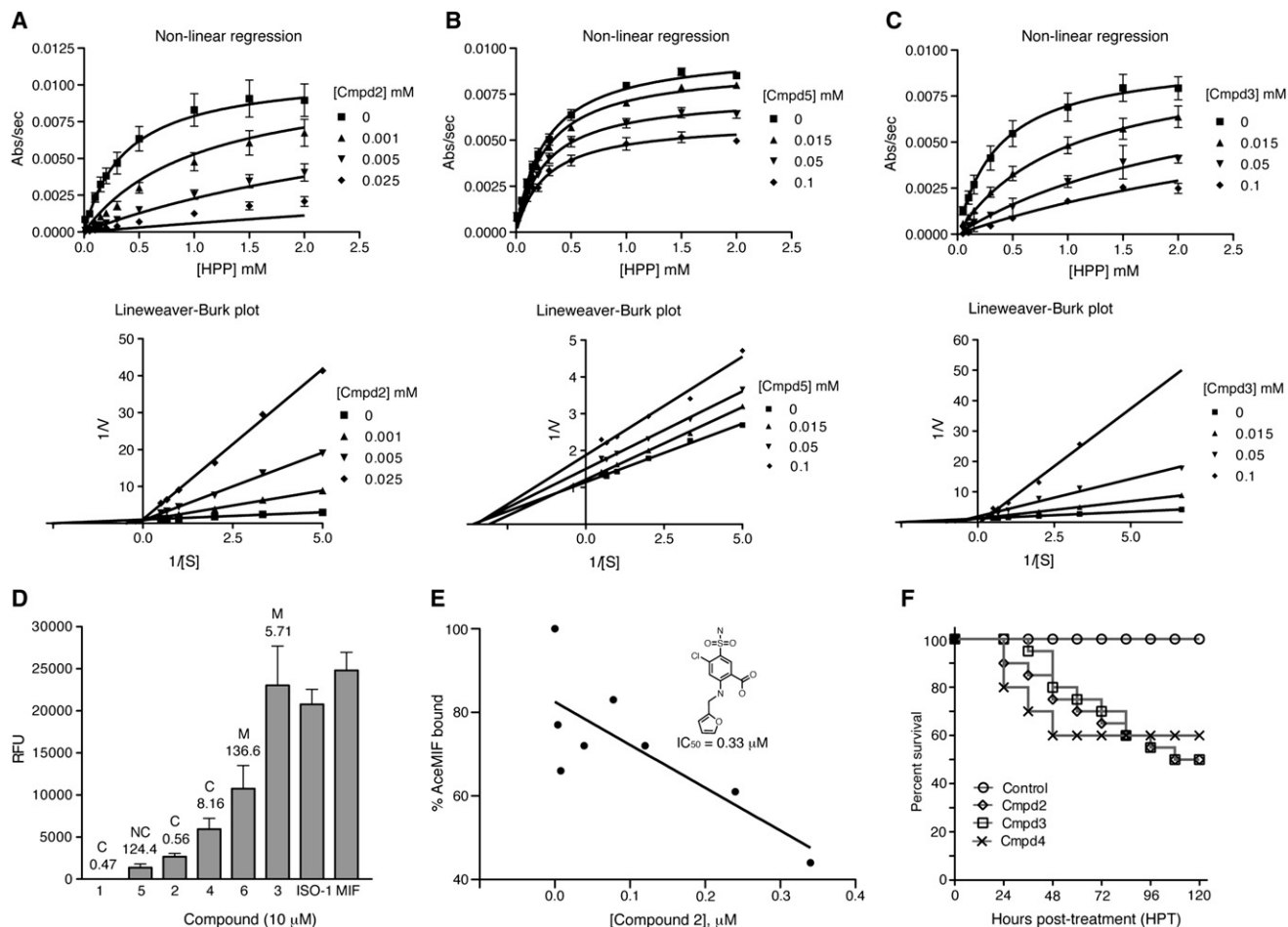


**Figure 2. Inhibition Assay against the Enzymatic and Biological Activity of AceMIF**

(A–C) Representative AceMIF hydroxyphenylpyruvate tautomerase inhibition of (A) compound 2 (competitive), (B) compound 5 (noncompetitive), and (C) compound 3 (mixed). Nonlinear regression of the initial velocity at various substrate and inhibitor concentrations is shown on the top panel, and Lineweaver-Burk plots are shown on the bottom panel for each inhibitor.

(D) PBMC migration inhibition assay with 8 nM AceMIF in the presence of 10  $\mu$ M compound concentration. Migrated cells were measured by relative fluorescence units (RFU) as described in [Experimental Procedures](#). The numbers above the bars are  $K_i$ 's (in  $\mu$ M) obtained from the tautomerase inhibition assay. One-letter codes above the numbers represent the type of enzymatic inhibition: C (competitive), NC (noncompetitive), and M (mixed).

(E) Inhibition of CD74-AceMIF interaction by compound 2. Percent of AceMIF bound to immobilized CD74 in the presence of various concentrations of compound 2 is plotted. Chemical structure of compound 2 is shown next to the plot. The  $IC_{50}$  value was determined based on the plot.

(F) Toxicity of AceMIF-specific inhibitors was determined by observing the survival of cultured *A. ceylanicum* adult worms. Only three of six compounds revealed worm-killing activity (>15% toxicity) at a dose of 100  $\mu$ M.

See also [Figure S1](#).

compound 13 increases the  $K_i$  102-fold relative to compound 2. The crystal structure of compound 2 indicates this linker is buried in the active site and replacing the amine proton with a methyl group would result a steric clash, destabilizing the interaction between inhibitor and AceMIF. Taken together, these results show that structural alterations of furosemide (compound 2) significantly impact the nature of their interaction with the AceMIF protein (and resulting inhibitory activities) and furosemide provides an excellent pharmacophore for novel anthelmintics.

#### NKCC1 Flux Assay

The diuretic activity of furosemide in humans makes it unsuitable as an anti-anthelmintic therapeutic for human use. To determine whether any of the furosemide analogs inhibited Na-K-Cl

symporter (NKCC1), a flux assay measuring the influx of  $^{86}\text{Rb}$  as a surrogate marker of  $\text{K}^+$  in the presence of furosemide and its structural analogs was measured ([Darman and Forbush, 2002](#)). Bumetanide was used as a positive control of inhibition. The assay was performed at 10  $\mu$ M and 100 nM concentrations of each compound. Only bumetanide and furosemide inhibited the  $^{86}\text{Rb}$  influx, whereas the furosemide analogs did not ([Figure 3](#)).

#### X-ray Crystallography

Attempts at cocrystallizing full-length AceMIF with the selected compounds in the original condition or in  $\sim 500$  commercial conditions were unsuccessful presumably caused by the crystal packing artifact in the apo crystal structure ([Figure S2](#)). Various

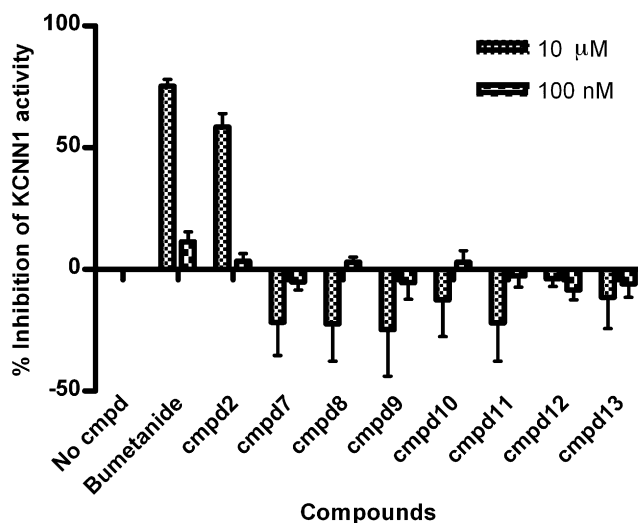
**Table 2. Crystallographic Data collection and Refinement Statistics**

	C2aMIF:Cmpd2	C2aMIF:Cmpd9
Data collection		
Space group	P3 <sub>1</sub> 21	P3 <sub>1</sub> 21
Cell dimensions		
a, b, c (Å)	86.8, 86.8, 115.5	86.2, 86.2, 114.9
(Alpha), (beta), (gamma) (°)	90, 90, 120	90, 90, 120
Resolution (Å)	1.8	2.1
R <sub>merge</sub>	0.088 (0.266) <sup>a</sup>	0.087 (0.447)
I/(sigma)I	5.2 (2.7)	8.1 (1.7)
Completeness (%)	94.3 (91.0)	100 (100)
Redundancy	8.8 (9.1)	10.4 (10.2)
Refinement		
Resolution (Å)	1.8	2.1
No. reflections	42,127	29,359
R <sub>work</sub> /R <sub>free</sub>	0.17/0.20	0.16/0.21
No. atoms		
Protein	2700	2697
Ligand/metal	123	86
Water	275	262
B-factors		
Protein	21.5	20.8
Ligand/metal	29.7	30.2
Water	30.6	29.6
Rmsd		
Bond lengths (Å)	0.033	0.028
Bond angles (°)	2.260	1.960

A single crystal was used for each structure.

<sup>a</sup>Highest resolution shell.

C-terminal truncations of AceMIF were tested for cocrystallization. Deletion of two C-terminal residues, Thr117 and Met118 ( $\Delta$ C2AceMIF), was the only truncation that resulted in cocrystals, diffracting at 1.8 Å in space group P3<sub>1</sub>21. The crystal structure was solved by molecular replacement and refined to R and R<sub>free</sub> of 17% and 20%, respectively. Electron density generated without a model of compound 2 shows the inhibitor in the active site in Figure 4A. The carboxylic acid oxygen (O4) of the anthranilate pharmacophore hydrogen bonds with the side chain hydroxyl group of Ser63, the backbone nitrogen atom of Ile64, and the side chain nitrogen atom of Lys32 (Figure 4B). The second carboxyl oxygen (O5) forms a hydrogen bond with the nitrogen atom of Pro 1, completing a tight hydrogen-bonding network with the hydrophilic residues in the active site. The sulfur atom of Met2 also hydrogen-bonds with the nitrogen of the furfurylamine group of compound 2. No water-mediated hydrogen-bonding interaction is visible in the electron density. Hydrophobic interactions exist between the furfuryl group and the residues consisting of one half of the active site (Figures 4A and 4B). The sulfonamide group and chloride atom are exposed to the solvent (Figures 4C and 4D). In contrast to the fully occupied active site by the furfuryl and carboxyl groups, there is an unoccupied site (Figures 4C and 4D) adjacent to the chloride atom, where chemical modifications can be made

**Figure 3. NKCC1 Flux Assay with Compound 2 and Its Structural Analogs**

Percent inhibition of <sup>86</sup>Rb influx into NKCC1 cotransporter-expressed HEK293 cells was measured in presence or absence of the compounds. Bumetanide was used as a positive control. The assay was performed at 10 μM and 100 nM compounds (n = 3). Most of the furosemide analogs exhibit negative inhibition and this is probably because of the low value of the untreated control cells located at the edge row of the assay plate.

to improve the affinity of this compound for AceMIF. This unoccupied site begins with a hydrophobic groove (Val106, Phe108, and Val113) and ends with hydrophilic residues (Asn109 and Thr112).

Compound 9 was also cocrystallized with  $\Delta$ C2AceMIF, and its X-ray diffraction data were collected at 2.1 Å (Figure 5 and Table 2). Compound 9 is a structural analog of compound 2 and lacks the solvent-exposed sulfonamide group and chloride atom. It has a 4-fold higher K<sub>i</sub> than that of compound 2. Crystal structures of AceMIF in complex with compounds 2 and 9 are superimposed using a maximum likelihood method (Theobald and Wuttke, 2006), with only protein C $\alpha$  atoms at the root-mean-square deviations (rmsd) of 0.11 Å and show an almost identical fit of the compounds in the active site (Figure 5C). The loss of the sulfonamide group and chloride atom from compound 2 results in a nondiuretic compound that retains its inhibition against AceMIF catalytic and migration activity.

## DISCUSSION

A previous report showed that AceMIF is secreted by adult hookworms and competes for binding to the human MIF receptor in vitro (Cho et al., 2007). Evidence also exists that protozoan (*Leishmania major* [Kamir et al., 2008]) and helminth (*Brugia malay* [Prieto-Lafuente et al., 2009]) parasite MIFs modulate host immune responses, presumably through interaction with mammalian receptors on immune cells. Moreover, the development of specific small molecule inhibitors synthesized to neutralize mammalian MIF has shown significant promise in their ability to ameliorate inflammatory disease (Al-Abed et al., 2005; Crichlow et al., 2007; Dabideen et al., 2007). The AceMIF

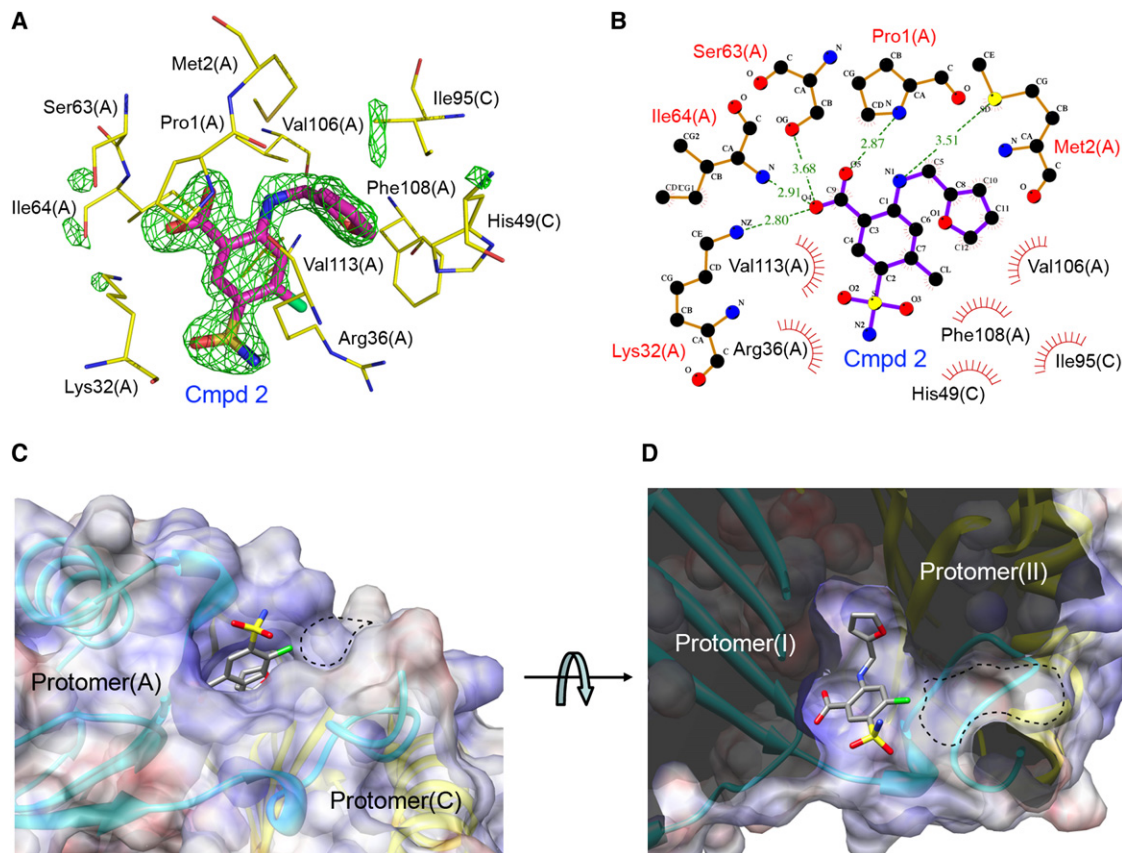


**Figure 4. Complex Crystal Structure with Compound 2**

(A) Difference in electron density of compound 2 was generated at  $3\sigma$  omitting the inhibitor in the final structure model.

(B) Interaction of compound 2 with active site residues. The residues involved in hydrogen-bond (ball and stick) and hydrophobic (spiked hemisphere) interactions are depicted. Hydrogen-bond distances are present on the green dashed lines.

(C) Compound 2 is shown on the electrostatic surface of AceMIF in an orientation pointing into the active site.

(D) A  $90^\circ$  rotation of panel (C).

In (C) and (D), the two protomers I and II forming the active site are represented in ribbons. The dotted area represents a protein site that could be used by novel analogs of the parent molecule to form new interactions, increasing the affinity for AceMIF and decreasing the affinity for carbonic anhydrase and the Na-K-Cl cotransporter.

See also Figures S2–S4.

vaccination experiment in this study shows that immunoneutralization provides partial protection to the host. The partial protection could potentially be explained by the presence of two MIF isoforms in *A. ceylanicum* (unpublished observation), which has also been demonstrated for other nematodes (Vermeire et al., 2008). It is possible that targeting both hookworm MIF proteins through vaccination or chemotherapy might further improve host protection. The human MIF tautomerase inhibitor, ISO-1, does not inhibit AceMIF catalytic nor macrophage migration activity, indicating the active sites are sufficiently different that a specific AceMIF small molecule inhibitor could be designed or discovered (Cho et al., 2007). Taken together, these studies support the rationale that targeting AceMIF represents a viable strategy to reduce hookworm pathogenesis and disease.

#### High Throughput Screening and Drug Repositioning

Among almost 1000 FDA-approved drugs or other bioactive compounds for the HTS screen, compounds that showed

$\geq 60\%$  inhibition of the *L*-dopachrome-methyl ester tautomerase activity of AceMIF in the initial screen were subjected to a more comprehensive analysis to characterize the  $K_i$ , which varied from submicromolar to hundreds of micromolar. The AceMIF-specific inhibitors identified in the HTS screen were characterized in other AceMIF assays. For example, plate-based chemotaxis and competition enzyme-linked immunosorbent assay experiments to probe the effect of inhibitor compounds on AceMIF-mediated cell migration and CD74 receptor binding were studied. Finally, all six compounds and selected analogs were tested to determine toxicity against *A. ceylanicum* in an ex vivo assay (Cappello et al., 2006). Only compounds 2, 3, and 4 (or their metabolites) demonstrated any worm-killing activity, which was clearly independent of any human target. Interestingly, compound 4 (pyrantel pamoate) is a neuromuscular depolarizing agent known to cause paralysis in helminthes, resulting in parasite expulsion through a mechanism involving inhibition of parasite cholinesterase. Identification of pyrantel



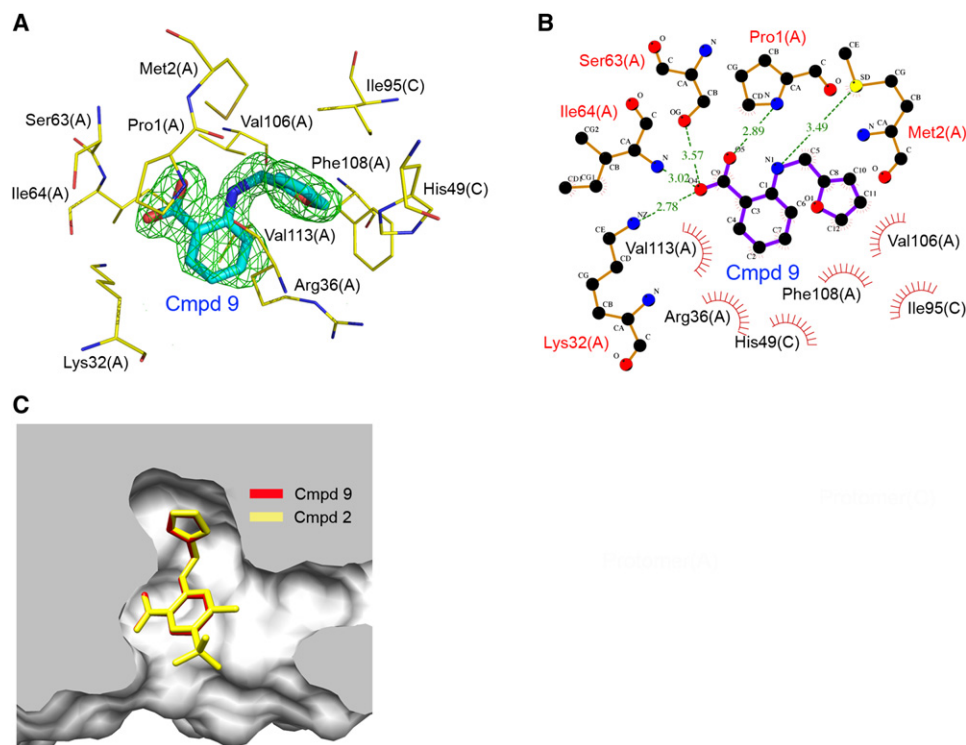


**Figure 5. Complex Crystal Structure with Compound 9, A Structural Analog of Compound 2**

(A) and (B) were generated in the same manner with those of compound 2 in Figure 3. (C) is the superposition of compounds 2 and 9 at the catalytic site. See also Figures S2 and S4.

pamoate as a specific inhibitor of AceMIF suggests this compound may have multiple targets within parasitic nematodes that are responsible for its anthelmintic properties. Among the six compounds that were identified, only compound 1 (sodium meclofenamate), an anti-inflammatory therapeutic that inhibits cyclooxygenase pathway (Matsell et al., 1994), might be repositioned as anthelmintic. The trough and peak levels of this drug are 0.2  $\mu\text{g/ml}$  and 15  $\mu\text{g/ml}$  (0.6  $\mu\text{M}$  and 45  $\mu\text{M}$ ), respectively, at an oral dose of 100 mg (Conroy et al., 1991). The trough level is higher than the  $K_i$  for catalytic activity, and 10  $\mu\text{M}$  of sodium meclofenamate would inhibit 100% of macrophage migration (Figure 1D and Table 1). The potential adverse effect of sodium meclofenamate includes impeding the immune system, which may prevent an appropriate response to hookworm infection. It is therefore very important to monitor the efficacy and adverse effects of compound 1 in the Syrian hamster model of hookworm disease and any future clinical trials in humans.

#### **$K_i$ and $\text{IC}_{50}$ for Receptor Binding, Macrophage Migration, and Hookworm Survival**

There was no strict interdependence among the  $K_i$  of enzymatic activity and  $\text{IC}_{50}$  values for receptor binding and chemotaxis inhibition. This paradox does not only involve the inhibitors in this study but also protein mutagenesis studies (Lubetsky et al., 2002; Swope et al., 1998) and mice knockin of a tautomerase null, Pro1-to-Gly MIF protein (P1G-MIF) replacing the endogenous *mif* gene (Fingerle-Rowson et al., 2009), that show a large decrease in catalytic activity and have a smaller decrease in bio-

logical activity. This suggests that protein-protein interactions are critical for the immunological function of MIF rather than the catalytic activity of MIF (Fingerle-Rowson et al., 2009). Taken together, these observations imply that MIF-receptor binding occurs at or near the tautomerase site and that some small molecule active site inhibitors have chemical moieties that interfere with the MIF-receptor interactions. In this regard, structural studies indicate that compound 2, which has a sulfonamide group and chloride atom that protrude from the active site and make no interaction with AceMIF, inhibits that interaction between AceMIF and human MIF receptor. These two groups are removed in compound 9. X-ray crystallography indicates that the interactions within the active site are retained, but this compound does not inhibit AceMIF-human MIF receptor interactions.

The ex vivo worm survival assay (at the single concentration of 100  $\mu\text{M}$ ) to test the toxicity of inhibitors to the parasite showed no clear relationship between inhibition of AceMIF enzymatic activity and *A. ceylanicum* killing. Again, this implies that the inhibition of the catalytic activity of AceMIF does not affect the pathology induced by the protein during hookworm infection. These incongruent results may be explained in part by the multifunctional nature of MIF proteins: (1) An active site that catalyzes a chemical reaction, and (2) a binding site near the active site that interacts with the MIF receptor. By selecting for inhibitors of tautomerase activity in the HTS, we have identified compounds effective in inhibiting the catalytic activity, including a few compounds that also disrupt MIF-receptor interactions.

### Pharmacophore Identification and Crystallographic Analysis

Compound 2 (furosemide) exhibited submicromolar  $K_i$  (0.56  $\mu\text{M}$ ) and  $\text{IC}_{50}$  (0.33  $\mu\text{M}$ ) values for the enzymatic and receptor binding inhibition activities, respectively, and inhibition of AceMIF-mediated monocyte chemotaxis ( $\text{IC}_{50}$  of 1  $\mu\text{M}$ ). In addition, it was also toxic to adult worms (50% killing relative to controls). Furosemide is a diuretic that blocks the Na-K-Cl cotransporter (Kirken-dall and Stein, 1968; Puschett, 1981). It has an anthranilate scaffold, as does meclofenamate, and can be represented by a benzene scaffold for a broader structural analog search. A furosemide-based search of commercially available reagents with decreased Tanimoto coefficients yielded seven structurally related compounds (compounds 7–13) to test the significance of each R-group (see Table 1) in AceMIF assays and in inhibiting the Na-K-Cl symporter. Kinetic assays revealed higher  $K_i$  values for all seven analogs, ranging from 5–247  $\mu\text{M}$  depending on the R-groups. Compounds 8 and 9 possessed similar activity to compound 2 in their ability to inhibit AceMIF-mediated PBMC migration (82% inhibition for both). Compound 8 also acts as an antagonist in solution with AceMIF, preventing its binding to CD74. However, none of the compound 2 analogs showed hookworm-killing activity, nor did any of the seven analogs inhibit the Na-K-Cl symporter.

Crystallographic analysis of compounds 2 and 9 complexed to AceMIF was performed to more fully understand the interaction of these compounds with AceMIF and to form the basis of future structure-based drug design studies. A superposition of the two structures is shown in Figure 5C and reveals an excellent overlay of the two compounds in the active site. The solvent accessible sulfonamide and chloride R-groups have no interactions with the protein for compound 2 and result in a marginal difference in  $K_i$  for compound 9, which does not contain either of these R-groups.

We also compared the crystal structures of AceMIF-compound 2 with human MIF-ISO-1 and with carbonic anhydrase-compound 2 to reveal the basis of these interactions (Figure S3). The specificity of the ISO-1 inhibitor for human MIF relative to AceMIF is based on different residues for one side (half) of the active site. In the carbonic anhydrase-compound 2 (PDB ID 1Z9Y) crystal structure (Puschett, 1981) the sulfonamide and the chloride make important binding interactions with carbonic anhydrase (Figure S4), whereas in the AceMIF co-complex these two R-groups point out of the active site into the solvent and make no interactions with the protein (Figure 4).

In summary, the AceMIF vaccination study provides the “proof-of-concept” for targeting a helminth immunomodulator with small molecule compounds. The high throughput screen identified six bioactive molecules. One AceMIF-specific inhibitor, sodium meclofenamate, could be repositioned as a hookworm therapeutic with the caveat that its adverse effects do not interfere with the immune response during treatment in animal model studies. Functional and structural studies of furosemide led to a pharmacophore and SAR studies. The differential effects of the compounds identified from the screen and the furosemide analogs will be useful in probing the relative significance of AceMIF-induced activities in the pathology of hookworm infection in vivo. This information will be useful for future structure-based drug design.

### SIGNIFICANCE

Hookworm disease is caused by intestinal, blood-feeding nematode parasites and infects nearly 600 million people worldwide, causing frequent morbidity, particularly in pregnant women and children. Reports of increasing treatment failure rates in human populations have raised concerns about potential anthelmintic resistance, especially against the benzimidazoles class of deworming drugs (Albonico et al., 2004). In the present study we screened a library of bioactive materials against an *Ancylostoma ceylanicum* homolog of macrophage migration inhibitory factor (AceMIF) and identified six inhibitors that could either be used as additional therapeutics for hookworm disease or scaffolds to design more potent compounds. Human MIF is a pro-inflammatory protein that has a variety of functions. AceMIF also possesses some of these functions, which may help the worm evade the host immune response by serving as a partial agonist for the MIF receptor. Six small molecule inhibitors of AceMIF were characterized for their effects on catalytic, receptor binding, and chemotactic activities of AceMIF. An ex vivo worm-killing assay was performed to test whether any of the HTS-identified inhibitors possessed anthelmintic activity. Some of these compounds already target hookworm disease by other mechanisms, which now may include inhibition of AceMIF function. Furosemide, a diuretic, exhibited the most potent combination of inhibitory activities relative to other identified compounds. Structure-activity studies of furosemide analogs lacking diuretic activity and crystallographic characterization of furosemide and a nondiuretic analog bound to AceMIF provide additional structural information that can be used to improve potency without reintroducing diuretic activity.

### EXPERIMENTAL PROCEDURES

Detailed experimental procedures can be found in Supplemental Experimental Procedures.

#### Materials

AceMIF was purified as described previously (Cho et al., 2007). HPP, L-3,4-dihydroxyphenylalanine methyl ester hydrochloride (methyl L-DOPA hydrochloride), and sodium (meta) periodate were purchased from Sigma (St. Louis, MO). Chemical analogs were obtained from Sigma, Ambinter (Paris, France), and the NCI/DTP Open Chemical Repository (<http://dtp.cancer.gov>).

#### AceMIF Immunization

For systemic immunization, groups of five male LVG hamsters (Charles River, Wilmington, MA) were immunized subcutaneously with 100  $\mu\text{g}$  of recombinant AceMIF protein using the adjuvant aluminum hydroxide (alum, Alohydrogel, HCl Biosector, Frederickssund, Denmark). Control animals were immunized with alum alone. The animals were to be boosted subcutaneously twice at 3 week intervals with the same dose. One week after the third immunization, hamsters were infected with 100 *A. ceylanicum* L<sub>3</sub> by oral gavage. For each of the vaccination groups studied, hamsters were weighed every other day and serum hemoglobin was measured using a commercially available kit (Sigma). Animals were followed for 40 days postinfection, and recombinant AceMIF protein-immunized animals were compared with adjuvant unimmunized and uninfected controls. For these studies, statistical analyses were carried out using the StatView, version 4.51, statistical software package (Abacus Concepts, Inc., Piscataway, NJ). Pairwise comparisons were performed using Student's *t* test. For multiple group comparisons, analysis of

variance was performed followed by Fisher's protected least significant difference as a posttest. P values of < 0.05 were considered significant.

#### High Throughput Screening for AceMIF Inhibitors

AceMIF was screened against a small chemical library at the Center for Chemical Genomics at Yale University. The Gen-Plus chemical library was obtained from MicroSource Discovery Systems Inc. and contains 960 bioactive compounds including marketed pharmaceuticals (Supplemental Experimental Procedures).

#### Measurement of $K_i$

The MIF keto-enol HPP isomerase activity was used to obtain  $K_i$  values for each inhibitor identified by HTS (Supplemental Experimental Procedures).

#### PBMC Migration Inhibition Assay

A preliminary peripheral blood mononuclear cell migration assay was performed as previously described (Cho et al., 2007) with one concentration of small molecule compounds (10  $\mu$ M) and one concentration of AceMIF (8 nM). Cell migration was assessed using the QCM chemotaxis 96 well assay (Chemicon, Billerica, MA). Fluorescence of migrated cells was measured using the 480/520 nm filter set of a Tecan Infinite M200 plate reader (Durham, NC). Results are graphically represented in relative fluorescence units (RFU) of experimental wells after subtraction of negative (no AceMIF) and background controls (no cells). A more comprehensive dose-response migration assay of PBMC chemotaxis was used to determine the  $IC_{50}$  of compound 2 (Figure S1).

#### MIF Receptor CD74 Capture Assay

Because of the sensitivity of the capture assay to DMSO, 10 mM of each compound in 100% DMSO was diluted to a final DMSO concentration of <0.04% DMSO before assaying. To elucidate CD74 inhibition by the compounds, a 96 well Immunoplate (NUNC, Rochester, NY) was coated with soluble CD74 ectodomain (sCD74<sup>73-232</sup>) as described (Leng et al., 2003). The inhibitors were preincubated with biotinylated AceMIF (2 ng/ $\mu$ l) prepared using the Biotin Labeling Kit (Roche Molecular Biochemicals, Nutley, NJ) for 1 hr at room temperature in the dark. Immobilized sCD74<sup>73-232</sup> was mixed and incubated with the preincubated inhibitor-biotinylated AceMIF at 4°C overnight. The plate was washed with 250  $\mu$ l/well Tween-20, Tris-buffered saline (Thermo Scientific, Pittsburgh, PA). The biotinylated AceMIF was detected by streptavidin-alkaline phosphatase (R&D Systems, Minneapolis, MN) followed by color development with 60  $\mu$ l/well of p-nitrophenylphosphate (Sigma) observed at 405 nm.

#### Toxicity against *A. ceylanicum* Ex Vivo

*A. ceylanicum* worms were removed from the small intestine of infected Syrian hamsters (Bungiro et al., 2001) and cultured in hookworm culture medium (HCM) consisting of RPMI 1640 medium, 50% FCS, 20 U/20  $\mu$ g/ml penicillin/streptomycin, 10  $\mu$ g/ml Fungizone (Bristol-Myers Squibb, New York, NY) as described (Cappello et al., 2006). The susceptibility of *A. ceylanicum* to AceMIF-specific inhibitors was evaluated by culturing wells of adult worms (10 worms/well, 2 wells/ treatment) in the presence of 100  $\mu$ M concentration of each compound. Control wells contained equivalent volumes of DMSO and/or albendazole (Sigma), the current standard for treating hookworm infections. At 24 hr intervals the wells were evaluated by light microscopy to determine the percentage of live vs. dead worms.

#### Structure-Activity Relationships

The structural similarity search was performed in the PubChem small molecule database of the National Center for Biotechnology Information (NCBI) with Tanimoto coefficients (structural similarity index) of 80 and 85. Seven structural analogs (compounds 7–13) of compound 2 were available for further studies (Table 1).

#### Flux Experiment

Target specificity of the furosemide analogs was tested against the Na-K-Cl cotransporter NKCC1 in a flux experiment as previously described (Darman and Forbush, 2002). In this study, we used low chloride hypotonic medium to preactivate NKCC1 for 40 min, then 20 mM  $Cl^-$  medium (135 mM NaCl, 5 mM  $K^+$ , 124 mM gluconate, 1 mM  $Mg^{2+}$ , 1 mM  $Ca^{2+}$ ) for a 10 min preincubation

with the testing compounds, and finally a 1.1-min flux in the regular flux medium, consisting of 135 mM NaCl, 5 mM RbCl, 1 mM  $CaCl_2/MgCl_2$ , 1 mM  $Na_2HPO_4/Na_2SO_4$ ,  $\sim 1 \mu Ci/ml$  86Rb, 10–4 M ouabain, and 15 mM NaHEPES, pH 7.4, without inhibitors and at two concentrations (10  $\mu$ M and 100 nM) of bumetanide, furosemide, and analogs.

#### X-ray Crystallography

The carboxyl terminal residues Thr117 and Met118 were truncated ( $\Delta C2$ AceMIF) to overcome a crystal-packing artifact that hinders cocrystallization of the selected inhibitors.  $\Delta C2$ AceMIF (32.5 mg/ml) was crystallized in complex with 2.5 mM of compound 2 or 9 in 0.1 M imidazole, pH 8.0, 0.16–0.24 M zinc acetate, and 15%–25% PEG3000. Crystals were grown to 400  $\mu$ m at 18°C within two weeks (Supplemental Data).

#### ACCESSION NUMBERS

The coordinates for the structure of AceMIF and furosemide complex is 3RF4 and for the structure of the AceMIF and compound 9 complex is 3RF5, and have been deposited in the Protein Data Bank.

#### SUPPLEMENTAL INFORMATION

Supplemental Information includes four figures, one table, and Supplemental Experimental Procedures and can be found with this article online at doi:10.1016/j.chembiol.2011.07.011.

#### ACKNOWLEDGMENTS

We thank the staff at the X29 beamline of National Synchrotron Light Source at the Brookhaven National Laboratory for assistance in data collection and are grateful to Dr. Biff Forbush for the flux assay. Financial support was provided by the National Institutes of Health grants R01 AI065029 (E.L.), R01 AI058980 (M.C.), R01 AI042310 (R.B.), F32 AI077267 (J.J.V.), and T32 NS007136 (Y.C.), and the Alliance for Lupus Research (R.B.). M.C. is a paid consultant and chief scientific advisor to Avix Technologies, LLC, a vaccine development company. Yale University has applied for a patent on AceMIF inhibition based on the described work in this manuscript.

Received: November 16, 2009

Revised: June 30, 2011

Accepted: July 8, 2011

Published: September 22, 2011

#### REFERENCES

- Al-Abed, Y., Dabideen, D., Aljabari, B., Valster, A., Messmer, D., Ochani, M., Tanovic, M., Ochani, K., Bacher, M., Nicoletti, F., et al. (2005). ISO-1 binding to the tautomerase active site of MIF inhibits its pro-inflammatory activity and increases survival in severe sepsis. *J. Biol. Chem.* 280, 36541–36544.
- Albonico, M., Engels, D., and Savioli, L. (2004). Monitoring drug efficacy and early detection of drug resistance in human soil-transmitted nematodes: a pressing public health agenda for helminth control. *Int. J. Parasitol.* 34, 1205–1210.
- Bernhagen, J., Krohn, R., Lue, H., Gregory, J.L., Zernecke, A., Koenen, R.R., Dewor, M., Georgiev, I., Schober, A., Leng, L., et al. (2007). MIF is a noncognate ligand of CXCR chemokine receptors in inflammatory and atherogenic cell recruitment. *Nat. Med.* 13, 587–596.
- Bethony, J., Brooker, S., Albonico, M., Geiger, S.M., Loukas, A., Diemert, D., and Hotez, P.J. (2006). Soil-transmitted helminth infections: ascariasis, trichuriasis, and hookworm. *Lancet* 367, 1521–1532.
- Bungiro, R., and Cappello, M. (2004). Hookworm infection: new developments and prospects for control. *Curr. Opin. Infect. Dis.* 17, 421–426.
- Bungiro, R.D., Jr., Greene, J., Kruglov, E., and Cappello, M. (2001). Mitigation of hookworm disease by immunization with soluble extracts of *Ancylostoma ceylanicum*. *J. Infect. Dis.* 183, 1380–1387.

- Cappello, M., Bungiro, R.D., Harrison, L.M., Bischof, L.J., Griffiths, J.S., Barrows, B.D., and Aroian, R.V. (2006). A purified *Bacillus thuringiensis* crystal protein with therapeutic activity against the hookworm parasite *Ancylostoma ceylanicum*. *Proc. Natl. Acad. Sci. USA* **103**, 15154–15159.
- Cho, Y., Jones, B.F., Vermeire, J.J., Leng, L., DiFedele, L., Harrison, L.M., Xiong, H., Kwong, Y.K., Chen, Y., Bucala, R., et al. (2007). Structural and functional characterization of a secreted hookworm Macrophage Migration Inhibitory Factor (MIF) that interacts with the human MIF receptor CD74. *J. Biol. Chem.* **282**, 23447–23456.
- Cho, Y., Crichlow, G.V., Vermeire, J.J., Leng, L., Du, X., Hodsdon, M.E., Bucala, R., Cappello, M., Gross, M., Gaeta, F., et al. (2010). Allosteric inhibition of macrophage migration inhibitory factor revealed by ibudilast. *Proc. Natl. Acad. Sci. USA* **107**, 11313–11318.
- Chong, C.R., and Sullivan, D.J., Jr. (2007). New uses for old drugs. *Nature* **448**, 645–646.
- Conroy, M.C., Randinitis, E.J., and Turner, J.L. (1991). Pharmacology, pharmacokinetics, and therapeutic use of meclofenamate sodium. *Clin. J. Pain* **7** (Suppl 1), S44–S48.
- Crichlow, G.V., Cheng, K.F., Dabideen, D., Ochani, M., Aljabari, B., Pavlov, V.A., Miller, E.J., Lolis, E., and Al-Abed, Y. (2007). Alternative chemical modifications reverse the binding orientation of a pharmacophore scaffold in the active site of macrophage migration inhibitory factor. *J. Biol. Chem.* **282**, 23089–23095.
- Dabideen, D.R., Cheng, K.F., Aljabari, B., Miller, E.J., Pavlov, V.A., and Al-Abed, Y. (2007). Phenolic hydrazones are potent inhibitors of macrophage migration inhibitory factor proinflammatory activity and survival improving agents in sepsis. *J. Med. Chem.* **50**, 1993–1997.
- Dagia, N.M., Kamath, D.V., Bhatt, P., Gupte, R.D., Dadarkar, S.S., Fonseca, L., Agarwal, G., Chetrapal-Kunwar, A., Balachandran, S., Srinivasan, S., et al. (2009). A fluorinated analog of ISO-1 blocks the recognition and biological function of MIF and is orally efficacious in a murine model of colitis. *Eur. J. Pharmacol.* **607**, 201–212.
- Darman, R.B., and Forbush, B. (2002). A regulatory locus of phosphorylation in the N terminus of the Na-K-Cl cotransporter, NKCC1. *J. Biol. Chem.* **277**, 37542–37550.
- de Silva, N.R., Brooker, S., Hotez, P.J., Montresor, A., Engels, D., and Savioli, L. (2003). Soil-transmitted helminth infections: updating the global picture. *Trends Parasitol.* **19**, 547–551.
- Esumi, N., Budarf, M., Ciccarelli, L., Sellinger, B., Kozak, C.A., and Wistow, G. (1998). Conserved gene structure and genomic linkage for D-dopachrome tautomerase (DDT) and MIF. *Mamm. Genome* **9**, 753–757.
- Fingerle-Rowson, G., Kaleswarapu, D.R., Schlander, C., Kabgani, N., Brooks, T., Reinart, N., Busch, R., Schutz, A., Lue, H., Du, X., et al. (2009). A tautomerase-null MIF gene knock-in mouse reveals that protein interactions and not enzymatic activity mediate MIF-dependent growth regulation. *Mol. Cell. Biol.* **29**, 1922–1932.
- Garside, P., and Behnke, J.M. (1989). *Ancylostoma ceylanicum* in the hamster: observations on the host-parasite relationship during primary infection. *Parasitology* **98**, 283–289.
- Guo, P., Hirano, M., Herrin, B.R., Li, J., Yu, C., Sadlonova, A., and Cooper, M.D. (2009). Dual nature of the adaptive immune system in lampreys. *Nature* **459**, 796–801.
- Hotez, P.J., Brooker, S., Bethony, J.M., Bottazzi, M.E., Loukas, A., and Xiao, S. (2004). Hookworm infection. *N. Engl. J. Med.* **351**, 799–807.
- Kamir, D., Zierow, S., Leng, L., Cho, Y., Diaz, Y., Griffith, J., McDonald, C., Merk, M., Mitchell, R.A., Trent, J., et al. (2008). A *Leishmania* ortholog of macrophage migration inhibitory factor modulates host macrophage responses. *J. Immunol.* **180**, 8250–8261.
- Kirkendall, W.M., and Stein, J.H. (1968). Clinical pharmacology of furosemide and ethacrynic acid. *Am. J. Cardiol.* **22**, 162–167.
- Kleemann, R., Hausser, A., Geiger, G., Mischke, R., Burger-Kentischer, A., Flieger, O., Johannes, F.J., Roger, T., Calandra, T., Kapurniotu, A., et al. (2000). Intracellular action of the cytokine MIF to modulate AP-1 activity and the cell cycle through Jab1. *Nature* **408**, 211–216.
- Leng, L., Metz, C.N., Fang, Y., Xu, J., Donnelly, S., Baugh, J., Delohery, T., Chen, Y., Mitchell, R.A., and Bucala, R. (2003). MIF signal transduction initiated by binding to CD74. *J. Exp. Med.* **197**, 1467–1476.
- Leng, L., Chen, L., Fan, J., Greven, D., Arjona, A., Du, X., Austin, D., Kashgarian, M., Yin, Z., Huang, X.R., et al. (2011). A small-molecule macrophage migration inhibitory factor antagonist protects against glomerulonephritis in lupus-prone NZB/NZW F1 and MRL/lpr mice. *J. Immunol.* **186**, 527–538.
- Lolis, E. (2001). Glucocorticoid counter regulation: macrophage migration inhibitory factor as a target for drug discovery. *Curr. Opin. Pharmacol.* **1**, 662–668.
- Lubetsky, J.B., Dios, A., Han, J., Aljabari, B., Ruzsicska, B., Mitchell, R., Lolis, E., and Al-Abed, Y. (2002). The tautomerase active site of macrophage migration inhibitory factor is a potential target for discovery of novel anti-inflammatory agents. *J. Biol. Chem.* **277**, 24976–24982.
- Matsell, D.G., Gaber, L.W., and Malik, K.U. (1994). Cytokine stimulation of prostaglandin production inhibits the proliferation of serum-stimulated mesangial cells. *Kidney. Int.* **45**, 159–165.
- McLean, L.R., Zhang, Y., Li, H., Choi, Y.-M., Han, Z., Vaz, R.J., and Li, Y. (2010). Fragment screening of inhibitors for MIF tautomerase reveals a cryptic surface binding site. *Bioorg. Med. Chem. Lett.* **20**, 1821–1824.
- Merk, M., Baugh, J., Zierow, S., Leng, L., Pal, U., Lee, S.J., Ebert, A.D., Mizue, Y., Trent, J.O., Mitchell, R., et al. (2009). The Golgi-associated protein p115 mediates the secretion of macrophage migration inhibitory factor. *J. Immunol.* **182**, 6896–6906.
- Mitchell, R.A., Liao, H., Chesney, J., Fingerle-Rowson, G., Baugh, J., David, J., and Bucala, R. (2002). Macrophage migration inhibitory factor (MIF) sustains macrophage proinflammatory function by inhibiting p53: regulatory role in the innate immune response. *Proc. Natl. Acad. Sci. USA* **99**, 345–350.
- Prieto-Lafuente, L., Gregory, W.F., Allen, J.E., and Maizels, R.M. (2009). MIF homologues from a filarial nematode parasite synergize with IL-4 to induce alternative activation of host macrophages. *J. Leukoc. Biol.* **85**, 844–854.
- Puschett, J.B. (1981). Sites and mechanisms of action of diuretics in the kidney. *J. Clin. Pharmacol.* **21**, 564–574.
- Roger, T., David, J., Glauser, M.P., and Calandra, T. (2001). MIF regulates innate immune responses through modulation of Toll-like receptor 4. *Nature* **414**, 920–924.
- Rosengren, E., Bucala, R., Aman, P., Jacobsson, L., Odh, G., Metz, C.N., and Rorsman, H. (1996). The immunoregulatory mediator macrophage migration inhibitory factor (MIF) catalyzes a tautomerization reaction. *Mol. Med.* **2**, 143–149.
- Rosengren, E., Aman, P., Thelin, S., Hansson, C., Ahlfors, S., Björk, P., Jacobsson, L., and Rorsman, H. (1997). The macrophage migration inhibitory factor MIF is a phenylpyruvate tautomerase. *FEBS Lett.* **417**, 85–88.
- Sato, A., Uinuk-ool, T.S., Kuroda, N., Mayer, W.E., Takezaki, N., Dongak, R., Figueroa, F., Cooper, M.D., and Klein, J. (2003). Macrophage migration inhibitory factor (MIF) of jawed and jawless fishes: implications for its evolutionary origin. *Dev. Comp. Immunol.* **27**, 401–412.
- Shi, X., Leng, L., Wang, T., Wang, W., Du, X., Li, J., McDonald, C., Chen, Z., Murphy, J.W., Lolis, E., et al. (2006). CD44 is the signaling component of the macrophage migration inhibitory factor-CD74 receptor complex. *Immunity* **25**, 595–606.
- Stephenson, L.S., Latham, M.C., and Ottesen, E.A. (2000). Malnutrition and parasitic helminth infections. *Parasitology Suppl.* **121**, S23–S38.
- Subramanya, H.S., Roper, D.I., Dauter, Z., Dodson, E.J., Davies, G.J., Wilson, K.S., and Wigley, D.B. (1996). Enzymatic ketonization of 2-hydroxymuconate: specificity and mechanism investigated by the crystal structures of two isomerases. *Biochemistry* **35**, 792–802.
- Sun, H.W., Bernhagen, J., Bucala, R., and Lolis, E. (1996). Crystal structure at 2.6-Å resolution of human macrophage migration inhibitory factor. *Proc. Natl. Acad. Sci. USA* **93**, 5191–5196.
- Suzuki, M., Sugimoto, H., Nakagawa, A., Tanaka, I., Nishihira, J., and Sakai, M. (1996). Crystal structure of the macrophage migration inhibitory factor from rat liver. *Nat. Struct. Biol.* **3**, 259–266.



Swope, M., Sun, H.W., Blake, P.R., and Lolis, E. (1998). Direct link between cytokine activity and a catalytic site for macrophage migration inhibitory factor. *EMBO J.* 17, 3534–3541.

Theobald, D.L., and Wuttke, D.S. (2006). THESEUS: maximum likelihood superpositioning and analysis of macromolecular structures. *Bioinformatics* 22, 2171–2172.

Vermeire, J.J., Cho, Y., Lolis, E., Bucala, R., and Cappello, M. (2008). Orthologs of macrophage migration inhibitory factor from parasitic nematodes. *Trends Parasitol.* 24, 355–363.

Zhang, J.H., Chung, T.D., and Oldenburg, K.R. (1999). A simple statistical parameter for use in evaluation and validation of high throughput screening assays. *J. Biomol. Screen.* 4, 67–73.